JCBPS; Section A; May 2018 – July - 2018, Vol. 8, No. 3; 469-491. E- ISSN: 2249 –1929
[DOI: 10.24214/jcbps.A.8.3.46991]

Journal of Chemical, Biological and Physical Sciences

An International Peer Review E-3 Journal of Sciences

*Available online at*www.jcbsc.org

Section A: Chemical Sciences

CODEN (USA): JCBPAT Research Article

Vitex agnus castus plant extract as Safe corrosion inhibitor for carbon steel 1018 in 1M hydrochloric acid

A.S. Fouda[1], G.Y.El-Ewady[1], H.M.El-Abbasy[2], S.M. Zidan[3]

[1] Chemistry department, Faculty of Science, Mansoura University, Mansoura, Egypt,
[2]Misr higher institute for Engineering & Technology Mansoura, Egypt
[3]General chemist at North & South Sinai for Water and wastewater holding company, Mansoura, Egypt

Received: 28 June 2018; **Revised:** 21 July 2018; **Accepted:** 29 July 2018

Abstract: The corrosion inhibition effectiveness of "Vitex agnus castus"(VAC) as corrosion inhibitor for carbon steel (CS) 1018 in 1.0 M HCl was confirmed using chemical and electrochemical methods. The data resulted from the measurements indicated that the inhibition efficiency (%IE) is dependent on both temperature and concentration of the extract. Tafel polarization (TP) data indicated that the extract behaves as mixed kind inhibitor. Langmuir's adsorption isotherm was found to be the best fit. Morphology of the surface was examined using scanning electron microscopy (SEM), Fourier transform infrared (FTIR) and atomic force microscopy (AFM) which confirmed the existence of a protective film of extract molecules on CS 1018 surface.

Keywords: Carbon steel, HCl, Vitex agnus castus extract, AFM, FTIR, SEM.

1. INTRODUCTION

Corrosion is a severe problem facing the world industrial projects, arising because of material interactions with the environment[1]. CS is one of the most widely used materials in the manufacture of industrial products because it shows excellent, low temperature toughness, hydrogen-induced crack and fracture resistances and a good weld ability. The atmospheric and natural corrosion of CS has always been of prime interest to different industries[2,3] Mineral acids, in concern, hydrochloric acid (HCl); has

been frequently used in manufacturing procedures such as acid cleaning, pickling and oil well acidizing. Such acids have shown strong corrosive environments for CS and as a result, the study of the prevention of steel corrosion is always a subject of high theoretical and practical interest[3]**.** Inhibitor**s** are compounds that suppress the rate of corrosion of metals by absorbing on the surface of the metals either through physical or chemical adsorption and thereby, change the structure of electrical double layer. The search for new and efficient corrosion inhibitors requires the clarification of interactions between inhibitor molecules and metal surfaces. In this concern, green corrosion inhibitors have been assumed to be suitable as ecofriendly in inhibiting severe corrosion attack which caused due to mineral acids existence with the metal surface, hence, retarding the redox reactions that takes place, as it shown greater inhibition that linked to the presence of electron donor atoms (heteroatoms) such as N,S,O,….etc. that containing lone pair of electrons or containing other clouds of Л electrons in aromatic rings, long carbon chain length as well as triple bond in their molecular structures that shared with the active sites on the CS surface during these redox reactions[5,6].

2. EXPERIMENTAL (Materials & Methods)

2.1 Plant material & Origin: Vitex agnus castus (VAC) plant belongs to the Verbenaceae family and is distributed throughout Mediterranean, Europe, central Asia, North Africa and the United States. The VAC plant has been also found and collected by many scientific Egyptian researchers from Saint Catherine, South Sinai at its flowering stage[7]. Traditionally, the fruits of this plant have been used as a herbal medicine for treatment of hormone disorders in women so that, the fruit extract is used for the treatment of severe premenstrual syndrome (PMS) and hot flashes associated with menopause[8,9].

2.2 plant preparation method: Firstly, the freshly VAC parts were taken to dry, grinded to powder and, 500 g of its powder was soaked in distilled water, boiling at 100°C and maintained for 48 h at room temperature. Then, the extract supernatant was taken away, filtered and put finally in two closed bottles with capacity 2 L as a stock solution from VAC extract , this stock has been stored[10,11] at 4 °C. Secondly, for preparing various concentrations for work, a one-gram equivalent (≈ 178 ml) from VAC stock solution was dissolved in 1L distilled water to achieve a diluted solution (1000 ppm) so that, a various concentration of (100,150,200,250,300) ppm were prepared from the latter dilution in order to be ready for work.

2.3 High Performance Liquid Chromatography (HPLC) analysis technique: The HPLC technique have been done under two (Standard/Official (ISO)) test methods: for Flavonoidal & Polyphenolic compounds, respectively[12-14] take 5 grams of investigated compounds and mixed them with methanol, centrifuged at 10^4 rpm for a time 60 sec. The resulted supernatant was then filtered over a 0.2 micro meter millipore membrane filter, thus, at that point 1-3 ml has been assembled in a vial for admission into a HPLC align 1200 arrangement supplied with auto-sampling injector, solvent degasser, ultraviolet (UV) detector set at 280 nm, 330 nm for phenols and flavonoids respectively and quaternary Hewlett Packard pump (series 1100). The column temperature was kept up at 35°C. Gradient separation was completed with methanol and acetonitrile as a mobile phase at flow rate of 1 ml/min. Retention time and peak area were introduced for the estimation of phenolic and flavonoids compounds interest by the information investigation of HP programming. For further study of the behavior of VAC as a medicinal plant towards corroded CS; the isolation of the active constituents from the aqueous VAC extract was made by the aid of both: The National Research Center (NRC) & the Food Technology Research Institute (FTRI) in the Agricultural Research Center (ARC) located in Dokki, Giza, Cairo. Isolation was made concerning on

both flavonoids & poly phenolic compounds from VAC extract as follows: - For Flavonoids, various compounds expressing in units (mg/100g) were; Luteolin-6-arabinose 8-glucose (1705.44) together with known flavonoid ones named after Casticin (Vitex carpin) [15, 54] and other essential oils[16,17]. Luteolin (Figure 1(b)) and its derivatives are common in edible plants used in traditional medicine for treating a wide variety of diseases, it has been reported to contain a strong anti-oxidative and anti-inflammatory activities[7,18]. As a result, The latter flavonoid compounds indicating the presence of mostly more glucose units that giving more existence of oxygen groups that consider to act as an active centers in which, it contain an electron donating groups causing blocked to the active sites on the CS surface that caused during the redox reaction and therefore, introducing a protective layer from VAC under investigation, which as a result, suppresses an aggressive corrosion that caused in the presence[19, 20] of 1M HCl. For the polyphenolic compounds which expressed in units (ppm) were: -Benzoic (3597.88), Caffeine (237.08). These polyphenolic compounds as well, indicated the presence of more oxygen donor atoms in their structure and more electron clouds around benzene rings from benzoic acid (**Figure 1**(a)), while in caffeine as another example (**Figure 1**(c)), in addition, more nitrogen donor atoms appear together with oxygen donor ones which then, assume to block the active sites by sharing its lone pair of electrons with d-orbital of iron on the carbon steel surface.

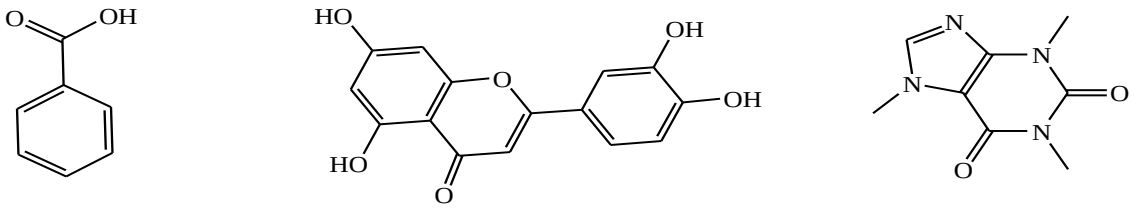

(a)Benzoic acid ($C_7H_6O_2$) (b) Luteolin ($C_{15}H_{10}O_6$) (c) Caffiene $C_8H_{10}N_4O_2$

Figure 1: Some Chemical Structures, molecular formulas examples of major constituents of HPLC flavonoidal and polyphenolic compounds which isolated from VAC extract

2.4 Weight loss method: The Weight loss (WL) study has been achieved by utilizing CS with composition (weight %): Mn 0.6, Si 0.003, C 0.2, P 0.04 and the rest[21] Fe. The solution (1M HCl) has been prepared from a reagent (HCl 36.5-38%) with twice distilled water, it was standardized using 1M Na_2CO_3) solution, so as to accurately adjust 1M HCl solution for work.

First of all, six CS 1018 specimens with dimensions (2cm x 2cm) were abraded well using emery paper of grades (120, 600,800,1200), respectively till the surface be shiny like a mirror, after that, all specimens were washed with acetone to remove impurities on metal surface, then washed by twice distilled water, finally, each specimen was dried between two filters papers & weighed (W_1) by using (sensitive Digital Balance :(AE-ADAM)- (pw 214)) with four decimal numbers.

Secondly, One of the CS coins has been immersed in 100 ml solution of 1M HCl to act as a blank , likely with the blank, the other five specimens were immersed in the latter solution, in addition of VAC extract solution of concentrations; 100,150,200,250,300 ppm were added for a time of 3h in a water bath [(Raypa)-(BAD-6)]which had been previously adjusted at temperature 25°C, then, all coins were excluded, splashed with twice distilled water ,dried gently and lastly weighed accurately, this will be

(W_2), the previous procedure steps have been repeated after raising temperatures to 30°C, 35°C, 40°C, 45°C, respectively.After recording the results in each temperature, the coverage of surface (θ) and the inhibition efficiency (%IE) had been measured utilized eq.(1)[22]:

$$\%IE = \theta \times 100 = (W_2 - W_1) / W_1 \times 100 \quad (1)$$

Where, the weight loss of CS specimens via an existence& non-existence of VAC inhibitor defined by W_2, W_1 respectively.

2.5 Electrochemical tests: The tests were carried out by utilizing three various methods, Tafel polarization (TP), AC impedance (EIS) & electrochemical frequency modulation (EFM). The electrochemical measurements, were achieved in aerated non-stirred 1 M hydrochloric acid solution at 25 °C together with concentrations (100,150,200,250,300 ppm) from VAC corrosion inhibitor. Solutions were freshly prepared from analytical grade chemical reagents using twice distilled water. The working electrode (WE) formed from one CS coin (1cmx1cm) soldered to a copper wire Preparing for an electric contact & inserted into glass tubes of suitable diameter by the aid of Araldite for introducing an effective surface of $1cm^2$ for contacting the test solution. Before each experiment, this WE was successfully abraded using gradually emery papers(600-1200)grades, degreased by acetone, rinsed by twice dist. H_2O and finally prepared to immerse in a conventional electrochemical cell (100 ml capacitance) which contain 3 compartments including CS 1018 as WE, platinum foil as auxiliary electrode (1 cm^2) & saturated calomel electrode (SCE) as reference electrode[23,24].

The values of cathodic (β_c) and anodic (β_a) Tafel constants were calculated from the linear region of the polarization curves &The corrosion current density (I_{corr}) was decided from the connection of the linear part of cathodic and anodic curves with stationary corrosion potential (E_{corr})[24,25].The corrosion current density (I_{corr}) was used in eq. (2)[21] in order to get the value of the inhibition efficiency (%IE) as follows :-

$$\%IE = \theta \times 100 = [1 - (I_{corr(inh)} / I_{corr(free)})] \times 100 \quad (2)$$

Where, $I_{corr(inh)}$ & $I_{corr(free)}$ are the currents in the presence and absence of VAC extract correspondingly.

(EIS) tests were done by AC signals of amplitude 5 mV peak to peak at the OCP through a frequency range (100 kHz and 0.2 Hz). EIS tests were verify at Open Circuit Potential (OCP) after inundation the electrode for half hour in the test solution**.** The obtained data from EIS was measure and deduced established by equivalent circuit. The %IE and (θ) gotten from the EIS are measured by following equation (3)[21]

$$\%IE = \theta \times 100 = [1 - (R^{\circ}_{ct} / R_{ct})] \times 100 \quad (3)$$

Where, R_{ct} , R°_{ct} represented charge transfer resistance via an existence and non-existence of extract, correspondingly

EFM was approved by utilizing 2 frequencies (2.0 & 5.0 Hz). Main frequency was 0.1 Hz, so, waveform repetitions after one second. Greater peaks were obtain to measure to EFM parameters[26] . All previous electrochemical measurements were performed utilizing Gamry PCI4-750 with Gamry Frame Work software. Echem Analyst 6.33 program has been selected to TP, EIS and EFM for data Fitting and calculating. Obtained results were assumed to be more accurate than previous WL measurements ones because, the electrochemical measurements have been done on recently prepared solutions[27,28].

2.6 Surface Analysis: Various investigations for surface topography of the CS exposed to 1M HCl solution with 300 ppm of the VAC extract were carried out by using (Scanning Electron Microscope : JOEL 840,Japan) with a magnifier power of (x1500) speed which located in The Faculty of Agriculture, Mansoura university. In the presence of 300 ppm of the VAC extract, the surface morphology of coins was also investigated using (Atomic Force Microscope: SPM 9600, dynamic (Non-contact) mode, shimadzu, Japan) which located in atomic force lab, Micro analytical center, Faculty of science, Cairo university. Lastly, specimen's surface were analyzed with FTIR affinity (Perkin Elmer) spectrophotometer that recording FTIR Spectra at central laboratory in faculty of pharmacy, Mansoura University. To perform surface analysis, the carbon steels were exposed to the test solutions for 24 h at 25˚C.

3. RESULTS AND DISCUSSION

3.1 Weight Loss Measurements

3.1.1 Adsorption isotherms: To provide better understanding of the adsorption of VAC inhibitor on the steel surface, several adsorption isotherms including Temkin, Freundlich, Bockris–Swinkels, Frumkin, Flory–Huggins and Langmuir were examined[29]. Normally, the best isotherm for a particular surface environment absorbent system is chosen by graphically fitting the experimental data to the adsorption equation[42]. After testing among the latter adsorption isotherm equations, the present calculations were fitted best to obey Langmuir 2nd equation, thus, by plotting previous concentrations of VAC inhibitor (C_{inh}) versus (C/ θ) and analyzing results, the adsorption formation constant (K_{ads}) was calculated according to Langmuir 2nd equation (equation 4)[30]:

$$C_{inh} / \theta = 1/ K_{ads} + C_{inh} \quad (4)$$

Where, K_{ads} =1/ intercept (Figure 2)

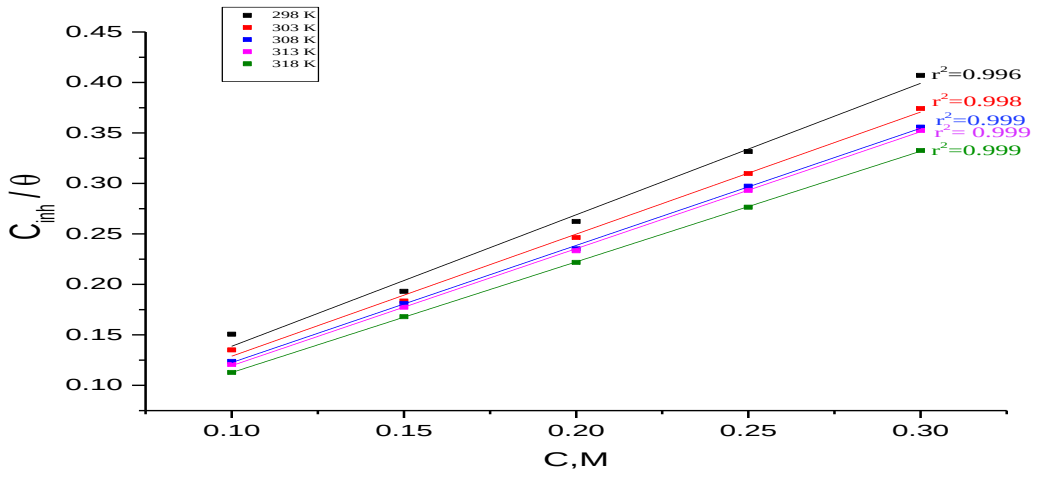

Figure 2: Langmuir adsorption plots of CS in 1M HCl in an existence & non-existence of different concentrations of VAC extract at different temperatures.

Figure 2 shows that, Langmuir 2nd equation was best fitted for previous calculations as it has described a good acceptance for weight loss results with a correlation coefficient (R^2) close to unity, therefore; ΔG^o_{ads} (standard Free Energy of adsorption) were calculated from [equation (5)][31]:

$$K_{ads} = 1 / 55.5 \exp(-\Delta G^{0}_{ads} /RT) \quad (5)$$

Where, R represent universal gas constant, T represents absolute temperature (Kelvin) & the (55.5) data implies H_2O concentration which involved in the solution bulk (mol /l).

Hence, by applying Vant Hoff's eq. (6)[32]

$$\log K_{ads} = (-\Delta H^{0}_{ads} /2.303\ RT) + \text{constant} \quad (6)$$

and plotting (log K_{ads}) vs. (1/T), we got value of the heat of adsorption (ΔH^{o}_{ads}) from slope where, slope = ($-\Delta H^{o}_{ads}$ /2.303 R).

The entropy (ΔS^{o}_{ads}), was finally been calculated from the basic thermodynamic principle equation (7)[31]:

$$\Delta G^{0}_{ads} = \Delta H^{0}_{ads} - T\Delta S^{0}_{ads} \quad (7)$$

After calculating, the latter results were tabulated accurately in (Table 1) as follows: -

Table 1: Thermodynamic parameters obtained from adsorption isotherm at different temperatures after 150 min immersion of VAC extract in 1M HCl solution

T, K	K_{ads} ,(g^{-1})	$-\Delta G^{\circ}_{ads}$, (kJ /mol)	ΔH°_{ads} ,(kJ/ mol)	$-\Delta S^{\circ}_{ads}$, (J/ mol. K)
298	118.1	21.7	43.7	219.7
303	125.6	22.3		217.8
308	152.9	23.2		217.1
313	273.9	25.1		219.7
318	321.5	25.9		218.8

The results of (Table 1), explained that, the negative sign of ΔG^{o}_{ads} indicating a spontaneous reaction, furthermore, data of ΔG^{o}_{ads} around -20 kJ mol^{-1} or smaller are consistent with the electrostatic interaction among the charged CS and the charged inhibitor (physisorption), while those more negative than -40 kJ mol^{-1} include electron transfer or sharing from the inhibitor particles to the surface of CS forming a coordinate type of bond (chemisorption).

So, ΔG^{o}_{ads} variation with temperature in the range from 21.7 to 25.9 kJ mol^{-1} exhibiting more physisorption process than chemisorption ones. unlikely, the ΔH°_{ads} calculated value were found to equal 43.7 kJ mol^{-1} with a positive sign indicating endothermic ones and as it slightly exceed 40 kJ mol^{-1} which assumed to be more physisorption than chemisorption since, it didn't exceed 100 kJ mol^{-1} which results in that, physical and chemical adsorptions are both involved[33].

However, entropy of formation ΔS^{o}_{ads} was found to decrease with a negative sign which indicated that , adsorption reaction is accompanied by an entropy reduction, Moreover, at the beginning of reaction, the

extract molecules might freely moving in the solution bulk (inhibitor molecules behaves chaotic) but ,with the adsorption progress, the inhibitor molecules were orderly aligned above CS surface leading to decrease in the disorder of such molecules resulted[34] in decreasing ΔS^{o}_{ads}.

3.1.2 Temperature influence: An influence of temperature on the CS corrosion via an existence & non-existence of various concentration of VAC has been studied by weight loss method. Wt. loss Vs. time for 250 ppm at different temperatures (25, 30, 35, 40, 45ºC) is shown in (Figure 4). The %IE from all concentrations at different temperatures are shown in (Table 2) which suggested that at 25ºC, as The VAC inhibitor concentrations increased, The active sites that formed during corrosion by 1M HCl on CS surface were blocked which then, increasing the adsorption of VAC molecules giving more surface coverage and as well, the inhibition efficiency increased till reaching optimum concentration (200 ppm)achieved higher %IE (77.1%).Furthermore, at (250 & 300 ppm) both concentrations of VAC inhibitor, a slightly desorption from the CS surface has happened leading to a gradually decrease in the inhibition efficiency as well .

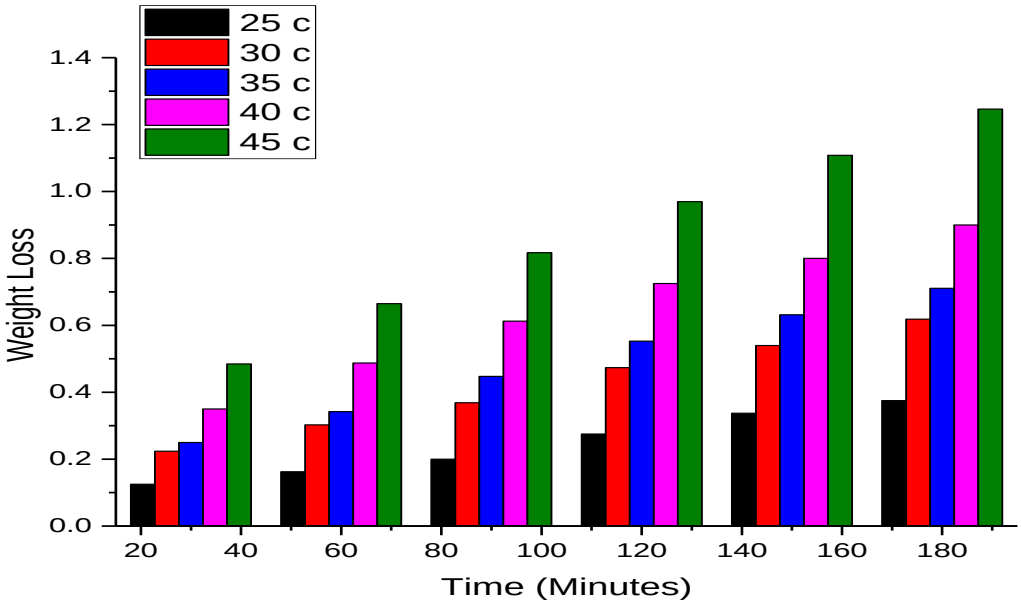

Figure 4: plots of WL vs time for 250 ppm concentration of VAC extract at different temperatures (25 - 45ºC)

The latter mechanism has been repeated by raising temperature from 30ºC till reached 45ºC which can be related to the fact that, higher temperatures might cause desorption of VAC from CS surface[33,35]. Besides ,experimental results in **(Table 2)** reveals an increase or decrease in the inhibitor efficiency depending on VAC concentration with raising temperatures suggested that , adsorption of inhibitor species above CS surface throughout such conditions was neither physical adsorption nor chemical ones but following an overall adsorption (physical and chemical adsorption)[36].

Table 2: % IE of different concentrations of VAC extract at different temperatures after 150 min immersion in 1 M HCl solution

Conc, ppm	%IE				
	25ºC	30ºC	35ºC	40ºC	45ºC
100	74.55	83.40	82.64	83.83	88.65
150	76.25	84.93	84.08	84.53	89.29
200	77.1	85.03	87.63	85.75	90.19
250	75.4	84.87	86.11	85.70	90.44
300	73.7	84.87	85.99	85.44	90.20

By further calculations concerning the transition State activation parameters (ΔH^*,ΔS^*, E^*_a) ,the apparent activation energy of reaction (E^*_a) were firstly obtained according to the Arrhenius equation (8)[37]:

$$\log k_{corr} = \log A - (E^*_a / 2.303\ R)\ 1/T \qquad (8)$$

Where k_{corr} is the rate of corrosion of metal & A represents pre –exponential factor. Plotting ($\log k_{corr}$) vs. (1000 / T) we got (E^*_a) value where, the slope will equal [$- E^*_a / 2.303$ R] (Figure 5).

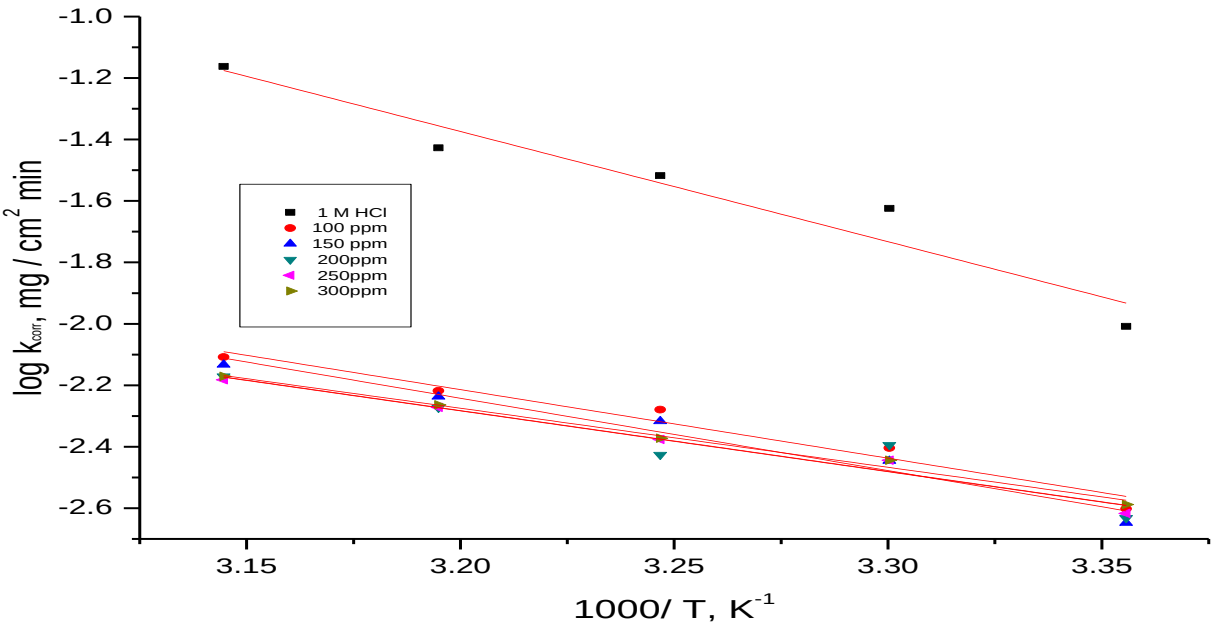

Figure 5: Arrhenius graph of CS in 1M HCl via an existence & non-existence in various concentrations of VAC inhibitor

In the same manner, the enthalpy & entropy of activation (ΔH^* & ΔS^*)respectively for activated complex formation in the transition state were obtained by plotting (log k_{corr} / T) vs. (1000/T) getting the both data of (ΔH^*), (ΔS^*) at different concentrations of VAC extract by using the transition state eq. (9) [37]and recording results accurately in (Table 3): -

$$\log k_{corr}/T = \log (R/Nh + \Delta S^*/2.303\ R) + (-\Delta H^*/2.303\ R)\ 1/T \quad (9)$$

whereas, (h) represents Plank's constant &(N) represents Avogadro′s number ,in which straight lines with intercept equal log (R/Nh +ΔS^* /2.303 R) and slope equal (- ΔH^*/ 2.303 R) were obtained (Figure 6).

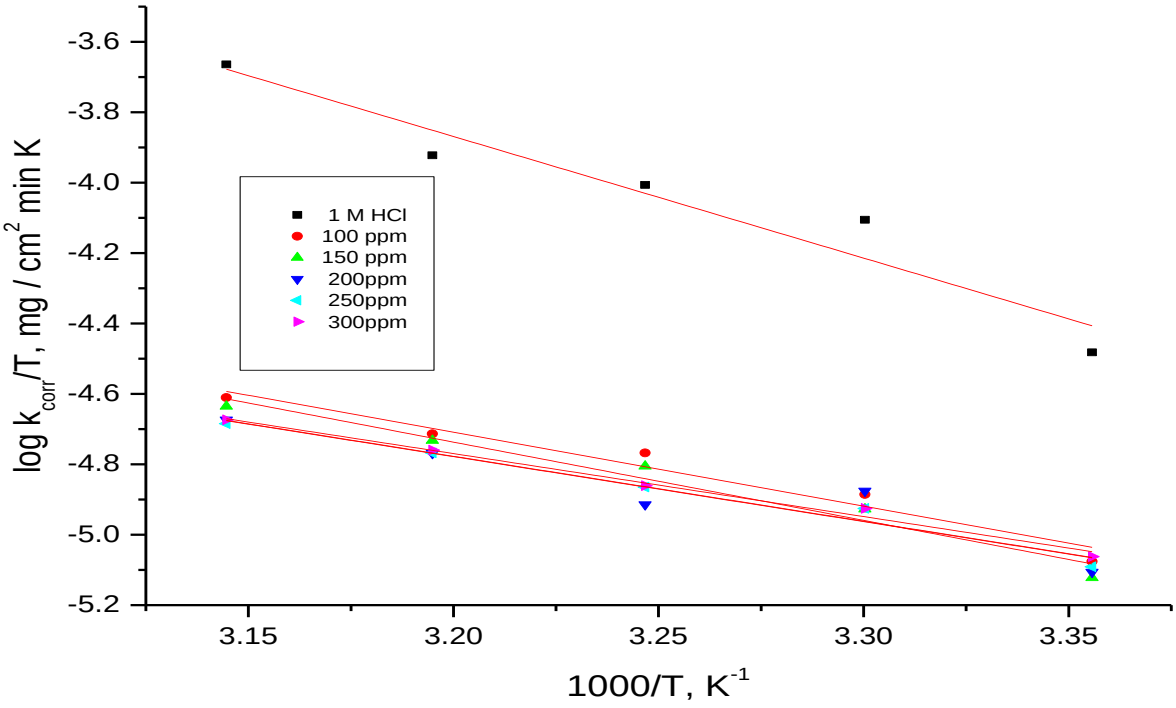

Figure 6 : Transition State plot of CS in 1M HCl via an existence & non-existence of different concentrations of VAC extract

Radovici[38] assort inhibitors into three groups depending on temperature influences:-

Firstly: -Inhibitors whose (% IE) decreases with the temperature increase, the apparent activation energy observed value was found greater than that in the uninhibited solution

Secondly: -Inhibitors whose (% IE) does not vary with temperature variation, the apparent activation energy does not affect with their absence or presence.

Thirdly: -Inhibitors whose (% IE) increases as temperature increase where, the observed value of $E_a^*$for the corrosion process is smaller than that obtained in the uninhibited solution. For the present obtained results in (Table 3), **the third group** was suggested to be the best fitted. in this case, the lower value of Ea^* in the solution with inhibitor compared with that without inhibitor is owing for its chemisorption,

while the opposite is the case with physical adsorption, this behavior was discussed on the basis that, such substances were strongly held on the metal surface, sometimes by chemisorption give arise to that, a surface film from the reaction product has formed & the metal′s surface area covered by inhibitor molecules increases as temperature raised. Therefore, the chemisorptive adsorption path is more likely[39]. This due to decrease rate of adsorption inhibitor with equilibrium data approach due to the tests at elevated temperatures according to Hoar & Holliday[40]. Otherwise, Riggs & Hurd[41] (explained that a decrease in E_a^* of corrosion at higher levels of inhibition originates from a movement of the net corrosion reaction from the unprotected part of the metal surface to the protected part). In addition, Schmid & Huang[42] obtained that, organic particles inhibit the both partial reactions (anodic & cathodic)above the surface of the electrode and a parallel reaction occur on the protected part, but the rate of reaction on the protected part is basically less than on the exposed part which gives an accord to the recent results[43].

Table 3: Transition state activation parameters for VAC extract after 150 min inundation in 1M HCl

Conc., ppm	E_a^*, (kJ /mol)	ΔH^*, (kJ /mol)	$-\Delta S^*$, (J /mol k)
1M HCl	**68.7**	**66.1**	**60.01**
100	**42.7**	**40.2**	**159.1**
150	**45.1**	**42.5**	**152.1**
200	**37.9**	**35.3**	**175.9**
250	**37.9**	**35.3**	**175.9**
300	**36.8**	**34.3**	**179.2**

The reaction enthalpy (ΔH^*)values was found to be positive as a sign for an endothermic nature and also strong ability of adsorption of VAC inhibitor on CS surface[44].Besides , as the activation energy (E^*_a) increased ,the enthalpy of the reaction(ΔH^*)decreases which synchronizing with VAC inhibitor that raised from lower to higher concentrations and that was explained according to the thermodynamic[45] relation $\Delta H^* = E_a^* - RT$. The entropy of reaction (ΔS^*) possess a negative charge values indicating that, activated complex in the rate determining step represents association process rather than dissociation ones[46], Moreover , (ΔS^*) has large values with increasing VAC concentrations from blank which demonstrates that, the system becomes ordered as VAC inhibitor was introduced with higher concentrations confirmed more orderliness as cleared in the higher inhibition efficiency compared to the lower concentrations[45].

3.2 Electrochemical tests

3.2.1 Tafel polarization tests: The (TP) diagrams (Figure 7) were listed for corrosion inhibition on the CS surface in 1.0 M HCl at different concentrations of the VAC plant extract in room temperature. The corrosion potential (E_{corr}), corrosion current (I_{corr}), the cathodic (β_c) & anodic (β_a) tafel slopes, (k_{corr}), (θ **)** and (%IE) were tabulated after calculations in (Table 4).

Table 4: Parameters obtained from TP on CS in 1M HCl with & without various concentrations of VAC extract at room temperature.

[Inh] Mg/L	$-E_{corr}$ mV vs SCE	$I_{corr,}$ µA /cm^2	β_c mV/dec	β_a mV/ dec	$k_{corr,}$ mpy	Θ	IE%
Blank	457	1190	153	96	550.0	-----	----
100	452	322	157	68	146.6	0.729	72.9
150	460	239	153	74	111.6	0.799	79.9
200	455	218	154	76	96.5	0.817	81.7
250	454	207	155	64	90.7	0.826	82.6
300	457	194	157	70	86.6	0.837	83.7

Data from (Table 4) showed that the cathodic Tafel slope (β_c) was shifted with a range of ± 4 mV from blank value where, for the anodic Tafel ones (β_a) was shifted with a range of 19± 7 mV from blank value which confirmed the view that, the VAC extract under investigation was capable of suppressing both the cathodic hydrogen evolution and the anodic CS dissolution by making a protective layer on the CS surface. In general words, VAC inhibitor was classified to be anodic or cathodic if the difference in (E_{corr}) value has been shifted to more than 85mv with respect to blank[47,48]. Therefore, there was no significant change observed in the corrosion potential (E_{corr}), as it recorded a minimum change of 5 mV which indicated the mixed type nature of VAC as an inhibitor. The corrosion current density (I_{corr}) was found to reduce from (1190 µA cm^{-2}) in blank to (194 µA cm^{-2}) when arrived at 300 ppm VAC extract that leading to %IE of 83.7%.

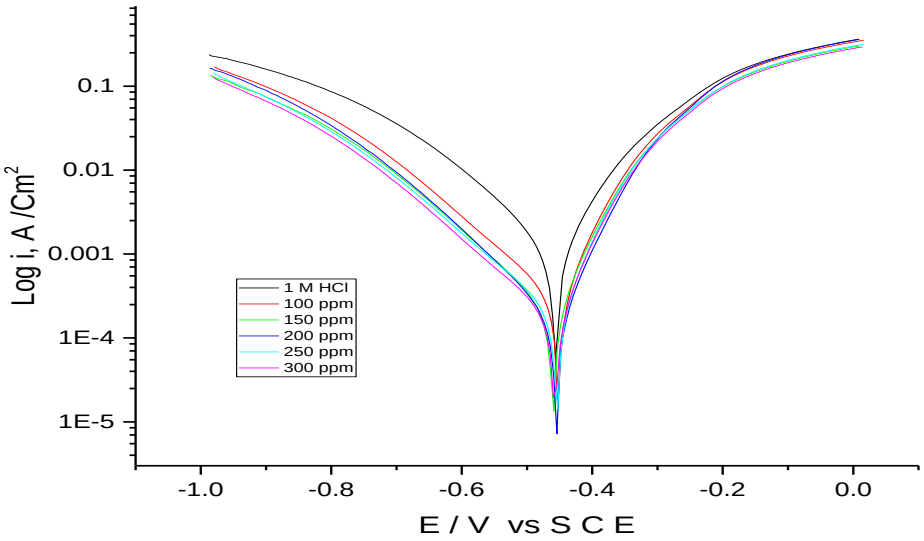

Figure 7: TP diagram of CS in 1 M HCl involving different concentrations of VAC extract at room temperature

3.2.2 EIS technique: EIS study has performed via the existence and non-existence of various concentrations of VAC extract. The Nyquist plots shown in (Figure 8) contains semicircles whose diameters rise with the concentration of the VAC extract, indicating the formation of a protective extract layer at the CS /solution interface. The results obtained in (Table 5) showed a significant increase in (R_{ct}) with the extract concentration because of the increased surface coverage. The extract addition leads to a reduction in the local dielectric constant and rise in the protective extract layer thickness at the electrode surface; this results in a decrease in C_{dl}. The Bode plots shown in (Figure 9)indicate the phase angle shift in the presence of the extract when compared to the uninhibited system, and a continuous increase is observed with the extract concentration. This is owing to the decrease in the dissolution of the metal and in the capacitive behavior on the electrode surface[49]. The EIS results were simulated using the equivalent circuit shown in (Figure 10). In the circuit, R_s signifies the solution resistance, R_{ct} represents the charge transfer resistance and *CPE* the constant phase element of double layer. The constant phase element consisting of Y_0 and n which are the admittance and exponent of *CPE*, respectively. In order to calculate the %IE and C_{dl}, eqs.10 & 11 were used, respectively

$$\%IE = [\,(R_{ct} - R^{\circ}_{ct} / R_{ct})\,] \times 100 \qquad (10)$$

$$C_{dl} = Y_0 (2\pi f_{max})^{n-1} \qquad (11)$$

so, (R_{ct})&(R°_{ct}) implying charge transfer resistances in presence and absence of the extract, correspondingly& f_{max} is the frequency at the maximum data. The decrease in the C_{dl} values could be discussed using equation (12)

$$C_{dl} = S^{\circ} S (s / d) \qquad (12)$$

Thus, (d) represents thickness for protective layer, (S°) represents permittivity of air, (S)is the local dielectric constant and (s)is the electrode surface area. The decrease in (C_{dl}) may reveals decreasing in the local dielectric constant or arise in thickness of the electrical double layer. Therefore, VAC extract particles may adsorb on the electrode surface through H_2O molecules replacement[50].

Table 5: EIS parameters for the corrosion of CS 1018 in 1M HCl with and without various concentrations of VAC extract in room temperature

[Inh], ppm	C_{dl} , μ Fcm^{-2}	R_{ct} , Ω cm^2	Θ	%IE
1 M HCl	1.133 x 10^{-4}	9.600	------	-----
100	8.936 x10^{-5}	22.57	0.575	57.5
150	7.827 x 10^{-5}	32.49	0.705	70.5
200	9.635 x 10^{-5}	36.14	0.734	73.4
250	8.619 x 10^{-5}	35.25	0.728	72.8
300	7.857 x 10^{-5}	37.97	0.747	74.7

From (Table 5), The corroding surface of the CS 1018 in 1 M HCl is expected to be heterogeneous because of its roughness, therefore; the parallel network (R_{ct}–C_{dl}) has considered to be a poor approximation, specifically for systems in which an efficient inhibitor is present.

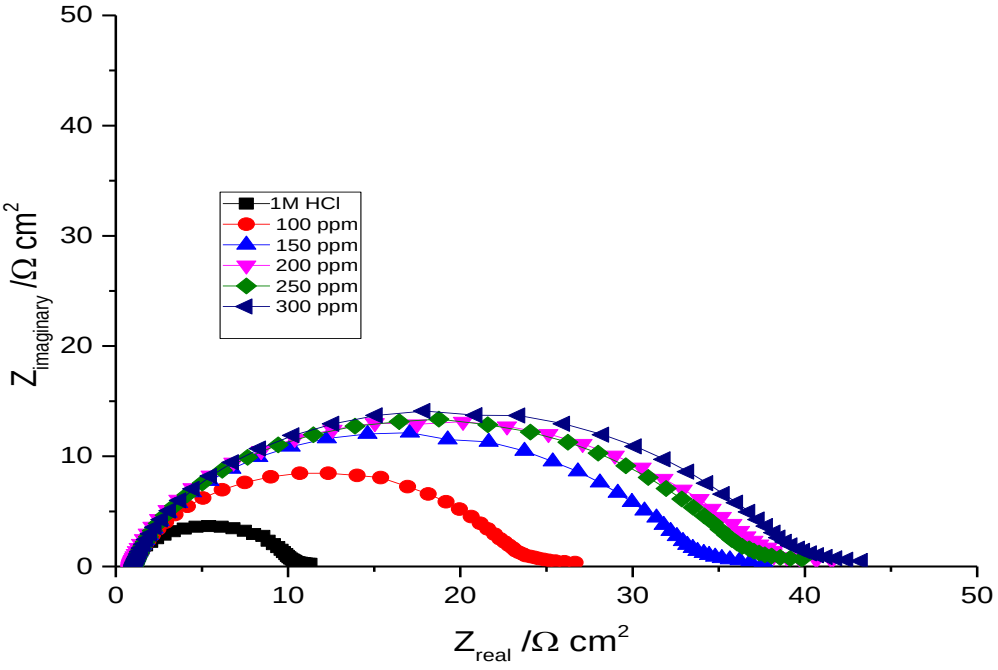

Figure 8: Nyquist plots for CS 1018 in 1 M HCl with various concentrations of VAC extract at 25°C

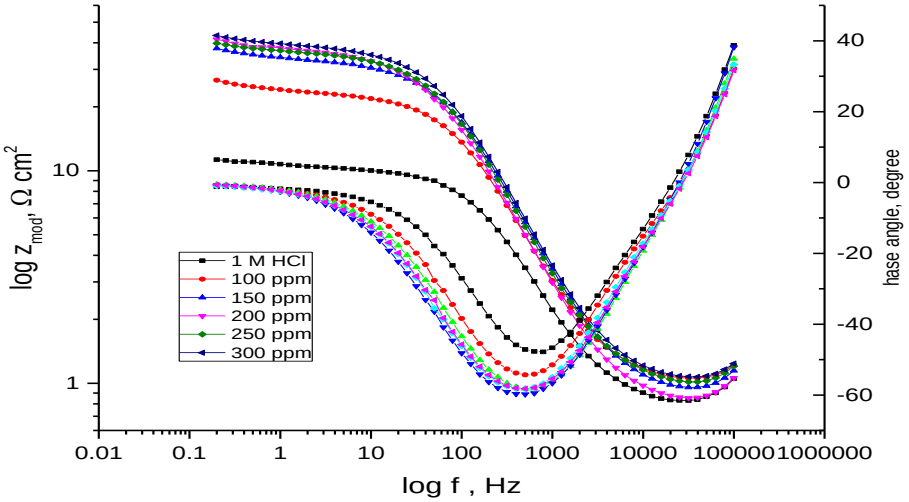

Figure 9: Experimental impedance and phase data in Bode format for CS in 1 M HCl including various concentrations of VAC extract denotes the fitted line using the Corresponding circuit.

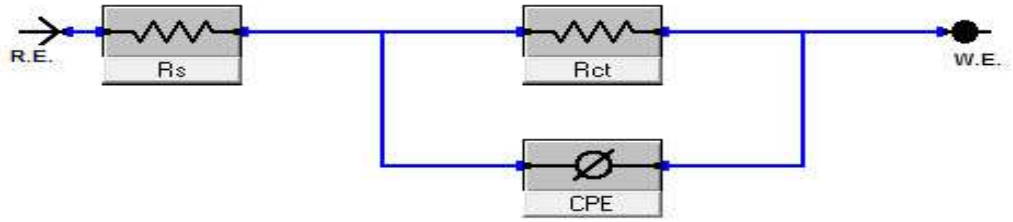

Figure 10: Corresponding circuit utilized for fitting EIS data

3.2.3 EFM technique: Data obtained in (Table 6) showed that, the current density (I_{corr}) decreased, which represent the corrosion rate (C.R.), by increasing the VAC extract concentrations, and hence, the surface coverage (Θ) increased that leads to a parallel increase in the %IE till reached to 86.4 % at concentration of 300 ppm. The causality factors according to experimental results are so close to those of theoretical (2.0 and 3.0) values which should confirmed the validity of Tafel slope and (I_{corr}) according to EFM theory, the causality factors results should indicated that the electrochemical measurement data were of good quality[25]. Hence, these data suggested that, VAC extract reduces the corrosion occurred on the CS 1018 surface through its mixed type nature (Figure 11).

Table 6:-parameters obtained by EFM for CS 1018 in 1M HCl solutions including different VAC concentrations in room temperature

[Inh] Mg/L	$i_{corr,}$ µA /cm^2	β_c, mV/ dec	β_a, mV /dec	Causality Factor -2	Causality Factor-3	k_{corr} , mpy	Θ	% IE
1M HCl	844.3	129	81	1.887	2.843	385.8	-----	-----
100	764.9	121	81	1.872	2.666	349.5	0.094	9.4
150	518.5	118	82	1.843	2.845	236.9	0.385	38.5
200	486.6	116	81	1.836	2.796	222.4	0.423	42.3
250	213.3	81	75	1.703	2.658	97.45	0.747	74.7
300	114.9	114	102	2.452	2.163	52.51	0.864	86.4

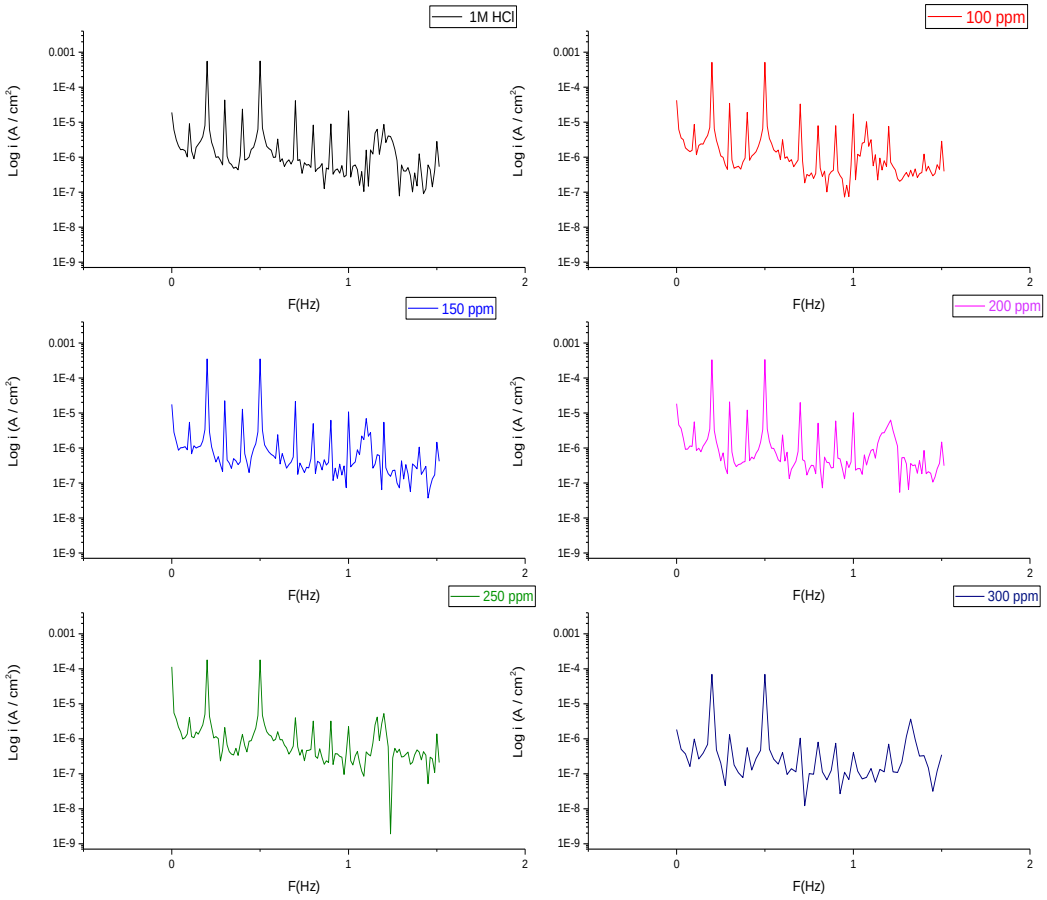

Figure 11: EFM spectra of CS 1018 in 1 M HCl including different concentrations of VAC extract at 25 °C

3.3 Surface Analytical Techniques

3.3.1 Scanning electron microscopy (SEM) tests: SEM was introduced for analyzing the CS surface morphology of CS after inundation in 1 M HCl during an existence and non-existence of VAC extract for 24 h at 25°C (Figure 12 (c)) A surface distortion was observed in the absence of VAC extract **(**Figure12 (b)) & that was due to the highly dissolution rate of iron at this pH. However, a thin and uniform layer on the surface of metal is observed in the presence of VAC extract. The cracks in the film are due to surface dehydration because the surface was dried prior to SEM imaging **(**Figure 12 (a)). In this concern, SEM picture results have expressed that VAC extract can be adsorbed on the CS surface which protects the surface from the acidic medium[51] of 1M HCl**.**

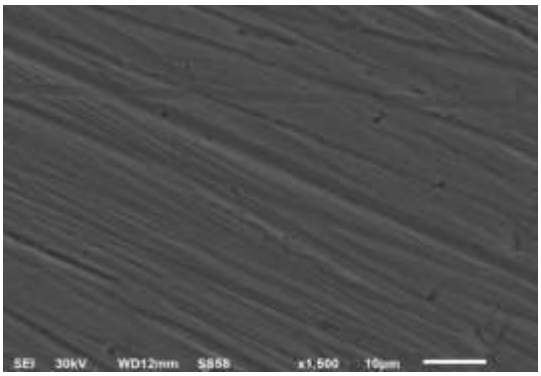

(a) Pure carbon steel

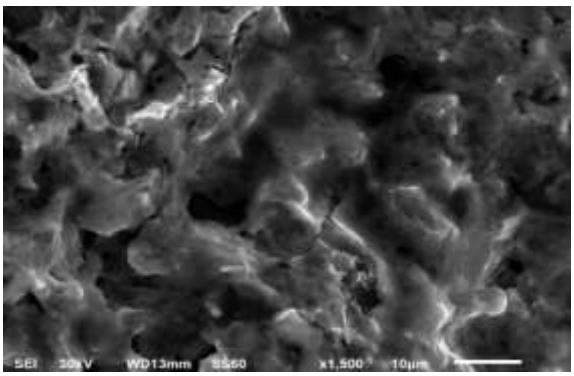

(b) blank (1M HCl)

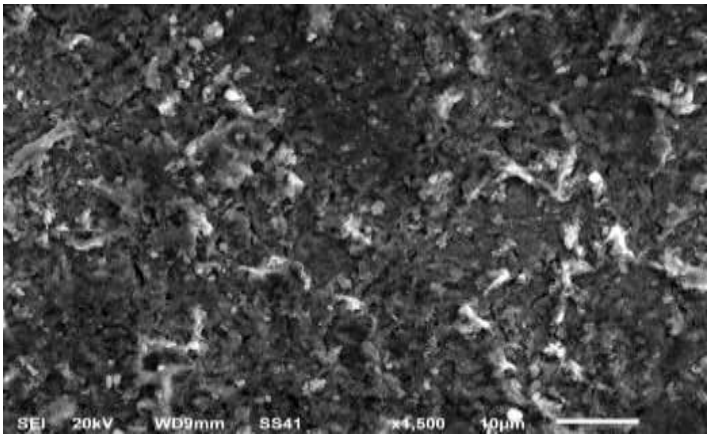

(c) Sample after 24 hrs immersion in 300ppm VAC

Figure 12: SEM micrographs of CS 1018 surface a) pure surface b) in 1M HCl c) after 24 hrs immersion in 300 ppm VAC extract with 1M HCl

3.3.2 Atomic force microscopy (AFM) tests: The AFM is considered the most fitted tool to measure surface topography as it able to provide three dimensional (3D) information on surface morphology[52]. It has been broadly used to measure the electrical properties of a sample at the nanoscale[53]. In the present work, AFM was employed to further investigate the effect of VAC extract on the corrosion of CS in acid solution. Two well-abraded CS specimens were degreased with acetone, double distilled water & lastly dried between two filter papers. AFM three-dimensional images obtained of the CS surface after 24 h of exposure to 1M HCl solutions with and without 300 ppm of VAC extract were shown in **(**Figure 13**)** in which, a relatively smooth and uniform surface morphology can be seen in the existence of VAC resulting a height of 596.83 nm **(**Figure 13 (b)**)**, whereas, the absence of VAC extract made the surface more rougher and distorted introducing a height of 1206.59 nm **(**Figure 13(a)). The roughness calculations were done using the (Gwyddion software, version 2.48, win 64-bit).Therefore,[The mean square roughness (RMS)] & [average surface roughness (R_a)] of CS surface in the 1M HCl solution without and with VAC extract were approximately equal to [47 µm, 36 µm] & [38 µm, 28 µm] respectively .In other words, low damage to the surface in case of 300 ppm VAC extract indicated that this extract is capable of introducing an effective corrosion inhibition[50,52,53] with1M HCl.

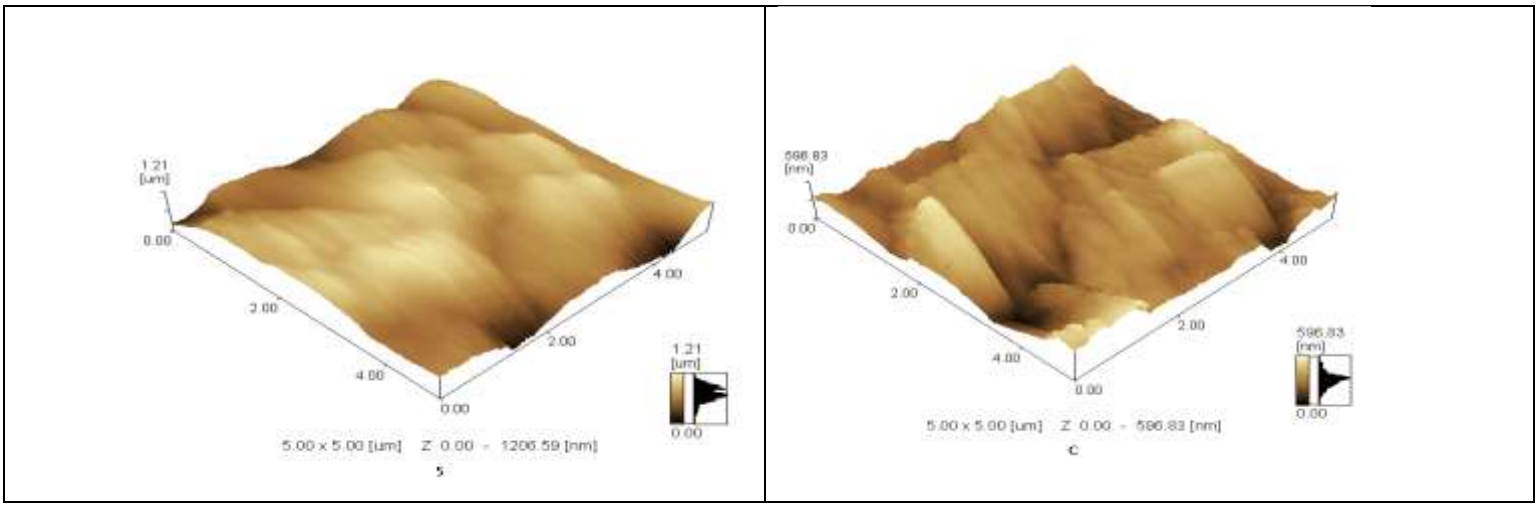

(a) Blank **(b**) After 24hrs immersion in 300ppm VAC

Figure 13: AFM images of CS surface a) in 1M HCl b) after 24 hrs. immersion in 300 ppm VAC extract with 1M HCl

3.3.3 Fourier transform infra-red spectroscopy (FTIR) tests: This powerful technique is defining the functional groups on the surface of CS. Reflectance infrared spectra were recorded in the range 4000 to 400 cm^{-1} (Figure 14).

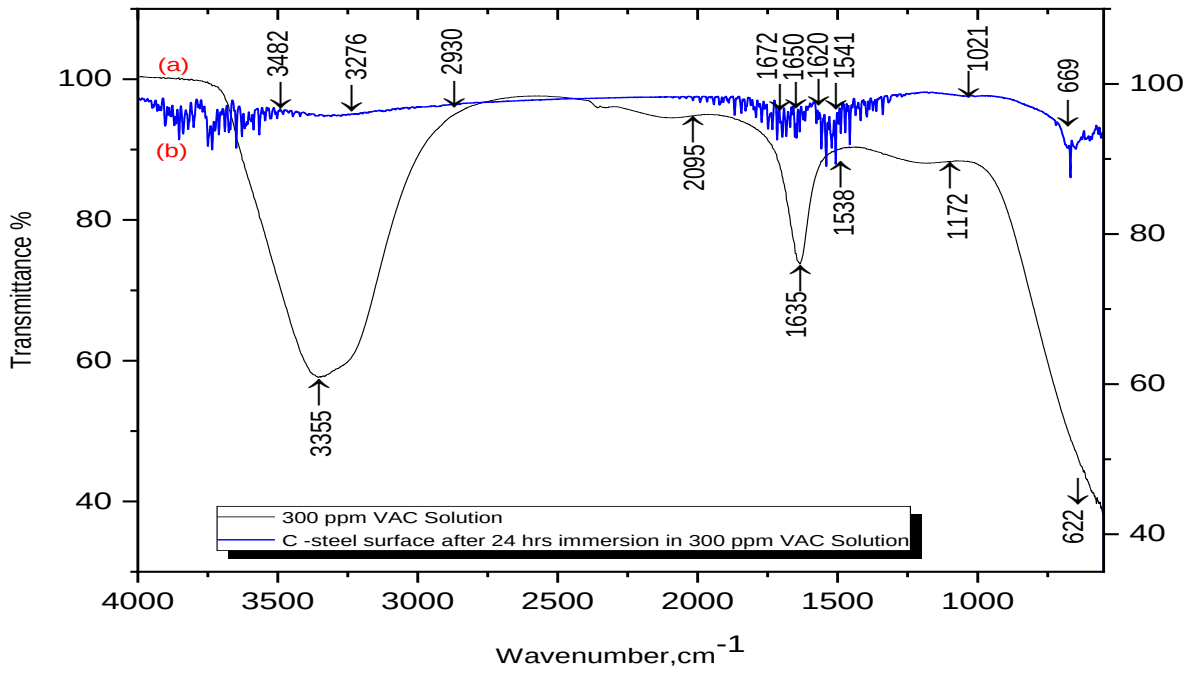

Figure 14: FT-IR spectra of :-(a) 300 ppm VAC extract, (b) CS surface after 24hrs immersion in the presence of 300ppm VAC extract with 1M HCl

Table 6: FT-IR spectral details of 300 ppm VAC extract and corrosion product on surface after 24hrs immersion with VAC extract solution together with 1M HCl

Observed Wave numbers (cm^{-1})		Frequency Assignment
300 ppm VAC Solution	Corrosion products / carbon steel / 1M HCl	
3355	3482	O-H /N-H stretch
---	3276	
2095	---	-C≡C- stretch
---	2930	C-H stretch
1635	1650	C=O stretch
	1672	
1538	1541	C-C in ring aromatics
---	1620	N-H bend
1172	1021	-C-O stretch
622	669	C-H bend

From **(**Figure 14**)** and analyzing results after tabulated it in **(**Table 6**), we** observed that the occurrence of a strong band at (3355 cm^{-1}) in the concentrated solution (300 ppm) of VAC extract (Figure 14 (a)**)** which, then shifted to two bands (3482 cm^{-1} & 3276 cm^{-1}) in the corrosion product that found on the carbon steel surface after 24 hours immersion with 1 M HCl **(**Figure 14(b)**)** which pertaining presence of (O-H /N-H)stretch. In addition, with the latter observed wave numbers, another peak at (2095 cm^{-1}) pertaining presence of (-C≡C-) stretch in the VAC solution, which disappears in the corrosion product. Whereas, it has found new band ones in the corrosion product at (2930 cm^{-1}) pertaining presence of (C-H stretch). The obvious peak in VAC solution at (1635 cm^{-1}) which then, after the reaction takes place has been shifted to two corresponding ones at (1650 &1672 cm^{-1}) lead us to an existence of a (-C=O) stretch, by further completion with those peaks, it has been found peak at (1538 cm^{-1}) in VAC solution which shifted to a corresponding peak at (1541 cm^{-1}) in the corrosion products reflects an existence of (C-C in ring aromatics).Furthermore, it has found a new band at (1620 cm^{-1})as an indication for (N-H bend).The peak at (1172 cm^{-1})has been downshifted to (1021 cm^{-1}) pertaining presence of (-C-O-) stretch. Finally, the peak at (622 cm^{-1}) in the extract was shifted to (669 cm^{-1}) in the corrosion products which lead us to (C-H bend) vibration.

All the previous resulting peaks in (Figure 14) indicated that, such missed wave numbers in the corrosion product indicating their participating in bonding. The shifting wave numbers and the new bond formation that appeared previously in (Table 6) through the functional groups of VAC inhibitor on the metal surface supporting the interaction between the active constituents of VAC inhibitor and the metal surface. The presence of extract components that containing nitrogen & oxygen heteroatoms together with Л electron clouds over benzene rings and other double and triple bonds finally confirmed that, those donor atoms and bonds act as active centers that suppresses the redox reaction by making a protective film from VAC solution through its mixed nature in adsorption so as to, inhibit severe corrosion which takes place with 1M HCl on the CS 1018 surface[56-61]**.**

4. CONCLUSIONS

VAC extract acts as an efficient corrosion inhibitor for CS 1018 in 1M HCl solution. The inhibition action of VAC extract has been attributed to a comprehensive adsorption through its HPLC major constituents. The VAC extract particles adsorbed above CS 1018 surface obeyed Langmuir adsorption isotherm. The %IE improved by improving the concentration of the extract molecules. Polarization curves indicated that, the extract molecules inhibit both anodic metal dissolution and also cathodic hydrogen evolution, so, VAC extract classified as mixed – type inhibitor. All electrochemical techniques are in good agreement with the obtained results. AFM, SEM & FTIR surface analytical techniques confirmed the formation of a protective layer from VAC extract on the CS surface.

REFERENCES

1. D.C. France, Anticorrosive influence of Acetobacter aceti biofilms on carbon steel ,J Mater Eng Perform, 2016, 25(9), 3580-3589.
2. Y. El Mendili, A. Abdelouas, and J.F. Bardeau Insight into the mechanism of carbon steel corrosion under aerobic and anaerobic conditions ,Phys Chem Chem Phys,2013, 15(23), 9197-204.
3. C.Verma, M. A. Quraishi, K. Kluza, M. Makowska-Janusik, L. O. Olasunkanmi, and E. E. Ebenso Corrosion inhibition of mild steel in 1M HCl by D-glucose derivatives of dihydropyrido [2,3-d:6,5-d'] dipyrimidine-2, 4, 6, 8(1H,3H, 5H,7H)-tetraone, Sci Rep,2017, 7, 44432.
4. T.Peme, L. O. Olasunkanmi, I. Bahadur, A. S. Adekunle, M.M. Kabanda and E. E. Ebenso, Adsorption and Corrosion Inhibition Studies of Some Selected Dyes as Corrosion Inhibitors for Mild Steel in Acidic Medium: Gravimetric, Electrochemical, Quantum Chemical Studies and Synergistic Effect with Iodide Ions,Molecules,2015, 20(9),16004-29.
5. N.O. Eddy, H. Momoh-Yahaya, and E.E. Oguzie , Theoretical and experimental studies on the corrosion inhibition potentials of some purines for aluminum in 0.1 M HCl,Journal of advanced research, 2015, 6(2), 203-217.
6. C.G. Dariva, and A.F. Galio, Corrosion inhibitors–principles, mechanisms and applications, in Developments in corrosion protection, InTech, 2014, ch.16.
7. N.M.Abdel-Hady, G.T. M. Dawoud , A. A. El-Hela , T. A. Morsy Interrelation of antioxidant, anticancer and antilieshmania effects of some selected Egyptian plants and their phenolic constituents, Journal of the Egyptian Society of Parasitology, 2011, 41(3),785-800.
8. M.Allahtavakoli, N. Honari, I. Pourabolli, M. K. Arababadi, H. Ghafarian, A. Roohbakhsh, A. E. Nadimi, and A. Shamsizadeh, Vitex Agnus Castus Extract Improves Learning and Memory and Increases the Transcription of Estrogen Receptor alpha in Hippocampus of Ovariectomized Rats, Basic Clin Neurosci,2015, 6(3), 185-92.
9. W.Wuttke, H.Jarry ,V. Christoffel ,B. Spengler, D. Seidlová-Wuttke, Chaste tree(Vitex agnus-castus) – Pharmacology and clinical indications, Phytomedicine, 2003, 10(4), 348-357.

10. A.Ahangarpour, A. A. Oroojan, L. Khorsandi, and S. A. Najimi , Pancreatic protective and hypoglycemic effects of Vitex agnus-castus L. fruit hydroalcoholic extract in D-galactose-induced aging mouse model, Research in Pharmaceutical Sciences, 2017, 12(2), 137-143.
11. A.Asdadi, A. Hamdouch, A. Oukacha, R. Moutaj, S. Gharby, H. harhar , El Hadek ,B. Chebli, L.M. I. Hassani , Study on chemical analysis, antioxidant and in vitro antifungal activities of essential oil from wild Vitex agnus-castus L. seeds growing in area of Argan Tree of Morocco against clinical strains of Candida responsible for nosocomial infections, J Mycol Med, 2015, 25(4), e118-e127.
12. Pirjo Mattila, Jouni Astola, and Jorma Kumpulainen, Determination of Flavonoids in Plant Material by HPLC with Diode-Array and Electro-Array Detections, Journal Agric.&food chem.2000, 48, 5834-5841.
13. Pascale Goupy, Mireille Hugues, Patrick Boivin and Marie Josephe Amiot, Antioxidant Composition and activity of barley (Hordeum vulgare) and malt extracts and of isolated phenolic Compounds, journal Sci.Food Agric.1999, 79, 1625-1634 .
14. F.B.El-kassas,A.M.Ali,S.E.Mostafa**,** Phenolic compounds as antioxidants of some product Manufactured from two cultivated Egyptian varieties of seedless grapes, Annals Agricultureal Sci, 2014,59,(2) 195-199.
15. M.G.Dodov, and S. Kulevanova, A review of phytotherapy of Acne vulgaris, Macedonian pharmaceutical bulletin, 2009, 55(1),2-8
16. C.Sarikurkcu, K. Arisoy , B. Tepe , A. Cakir , G. Abali , E. Mete, Studies on the antioxidant activity of essential oil and different solvent extracts of Vitex agnus castus L. fruits from Turkey, Food and Chemical Toxicology,2009, 47(10), 2479-2483.
17. S.N.Chen, J. B. Friesen, D.Webster, D. Nikolic, R.B.V. Breemen, Z. J. wang,H.H.S. Fong, N.R. Farnsworth and G.F. Pauli, Phytoconstituents from Vitex agnus-castus fruits,Fitoterapia,2011, 82(4),528-533.
18. M.I. Choudhary, Azizuddin , S. Jalil, S. A. Nawaz,K. M. Khan,R. B. Tareen,Atta-ur-Rahman Antiinflammatory and lipoxygenase inhibitory compounds from vitex agnus-castus, Phytotherapy Research, 2009, 23(9),1336-1339.
19. C.Hirobe, ZS. Qiao, K. Takeya, H. Itokawa, Cytotoxic flavonoids from Vitex agnus-castus, Phytochemistry, 1997, 46(3), 521-4.
20. Z.Hajdu, J. Hohmann , P. Forgo, T. Martinek , M. Dervarics , I. Zupkó, G. Falkay , D. Cossuta , I. Máthé, Diterpenoids and flavonoids from the fruits of Vitex agnus-castus and antioxidant activity of the fruit extracts and their constituents, Phytother Res, 2007, 21(4), 391-4.
21. A.S. Fouda ,K.Shalabi, Y.M. Abdallah, Hala M. Hassan, Adsorption and corrosion inhibition of Atropa belladonna extract on carbon steel in 1 M HCl solution ,Int. J. Electrochem. Sci, 2014, 9(3).
22. S. Fouda,M.Abdallah, S.A. Shama and E. A. Afifi, Azodyes as corrosion inhibitors for dissolution of c-steel in hydrochloric acid solution ,African Journal of Pure and Applied Chemistry,2008, 2(9), 083-091.

23. S.K.Saha, A. Dutta , P. Ghosh, D. Sukul , P. Banerjee, Novel Schiff-base molecules as efficient corrosion inhibitors for mild steel surface in 1 M HCl medium: experimental and theoretical approach, Phys Chem Chem Phys,2016, 18(27), 17898-911.
24. M.N.El-Haddad, Chitosan as a green inhibitor for copper corrosion in acidic medium, Int J Biol Macromol, 2013, 55, 142-9.
25. A.S. Fouda, A.Y. El-Khateeb, I. Mousa, M. Fakih , Adhatoda aqueous plant extract as environmentally benign corrosion inhibitor for carbon steel in sanitation water in polluted NaCl solutions and its biological effect on bacteria ,Nature and Science,2015, 13, 71-82.
26. K.Li, B. Wang , B. Yan ,W. Lu, Microstructure, in vitro corrosion and cytotoxicity of Ca-P coatings on ZK60 magnesium alloy prepared by simple chemical conversion and heat treatment,J Biomater Appl,2013, 28(3), 375-84.
27. S.Junaedi, AA. Al-Amiery, A. Kadihum ,AA. Kadhum ,AB. Mohamad, Inhibition effects of a synthesized novel 4-aminoantipyrine derivative on the corrosion of mild steel in hydrochloric acid solution together with quantum chemical studies, Int J Mol Sci,2013, 14(6),11915-28.
28. K.Shalabi, and A.A. Nazeer , Adsorption and inhibitive effect of Schinus terebinthifolius extract as a green corrosion inhibitor for carbon steel in acidic solution, Protection of Metals and Physical Chemistry of Surfaces, 2015, 51(5),908-917.
29. M.Abdallah, and M.E. Moustafa, Inhibition of acidic corrosion of carbon steel by some mono and bis azo dyes based on 1,5 dihydroxynaphihalene,Annali di chimica, 2004, 94(7-8), 601-11.
30. A.Y.El-Etre , Inhibition of acid corrosion of carbon steel using aqueous extract of olive leaves, J Colloid Interface Sci,2007, 314(2), 578-83.
31. A.S. Fouda, K. Shalabi, and A. E-Hossiany, Moxifloxacin antibiotic as green corrosion inhibitor for carbon steel in 1 M HCl, Journal of Bio-and Tribo-Corrosion, 2016, 2(3),1-13.
32. R.Kamaraj,P. Ganesan,J. Lakshmi,S.Vasudevan, Removal of copper from water by electrocoagulation process--effect of alternating current (AC) and direct current (DC), Environ Sci Pollut Res Int,2013, 20(1), 399-412.
33. E.E.Ebenso,I.B.Obot , Inhibitive properties, thermodynamic characterization and quantum chemical studies of secnidazole on mild steel corrosion in acidic medium, Int. J. Electrochem.Sci, 2010, 5, 2012-2035
34. S.A.Umoren and I.B.Obot, Polyvinylpyrollidone and polyacrylamide as corrosion inhibitors for mild steel in acidic medium, Surface Review and Letters,2008, 15(03), 277-286.
35. F.Bentiss, M. Traisnel, N. Chaibi, B. Mernari, H. Vezin and M. Lagrenee, 2,5-Bis(n-methoxyphenyl)-1,3,4-oxadiazoles used as corrosion inhibitors in acidic media: correlation between inhibition efficiency and chemical structure, Corrosion science,2002, 44(10), 2271-2289.
36. E.A.Noor, Temperature Effects on the Corrosion Inhibition of Mild Steel in Acidic Solutions by Aqueous Extract of Fenugreek Leaves,International Journal of Electrochemical Science, 2007, 2(12) ,1452-3981.

37. A.S. Fouda, K. Shalabi and A.A.Nazeer , Corrosion inhibition of carbon steel by Roselle extract in hydrochloric acid solution: electrochemical and surface study, Research on Chemical Intermediates,2015, 41(7), 4833-4850.
38. O. Radovici, Proceedings of the 2nd European Symposium on Corrosion Inhibitors, Ferrara, Italy, 1965, 178.
39. F.M.Mahgoub, F.M. Al-Nowaiser, and A.M. Al-Sudairi, Effect of temperature on the inhibition of the acid corrosion of steel by benzimidazole derivatives,Protection of Metals and Physical Chemistry of Surfaces,2011, 47(3),381.
40. T.P. Hoar, R.D.Holliday, The inhibition by quinolines and thioureas of the acid dissolution of mild steel, J. Appl. Chem.,1953, 3(11),502.
41. O.L. Riggs Jr., R.M.Hurd, Temperature Coefficient of Corrosion Inhibition, Corrosion, 1967, 23(8),252.
42. G.M. Schmid, H.J. Huang, Spectro-electrochemical studies of the inhibition effect of 4,7-diphenyl -1,10-phenanthroline on the corrosion of 304 stainless steel, Corros. Sci., 1980, 20(8-9), 1041.
43. A.S. Fouda, O.A. El Gammal, A.A. Hassan, S.M. Taha, Studies on the inhibition of corrosion of carbon steel in acidic solutions using some thiosemicarbazide derivatives, Der pharma chemica,2016, 8(2),318-331.
44. M.P. Chakravarthy, K.N. Mohana, C.B.Pradeep Kumar and A.M. Badiea, Corrosion Inhibition Behaviour and Adsorption Characteristics of Dapsone Derivatives on Mild Steel in Acid Medium, American Chemical Science Journal, 2015, 8(2), 1-16.
45. S. Umoren,M. M. Solomon,A. U. Israel,U.M. Eduok &A. E. Jonah, Comparative Study of the Corrosion Inhibition Efficacy of Polypropylene Glycol and Poly (Methacrylic Acid) for Mild Steel in Acid Solution,Journal of Dispersion Science and Technology, 2015, 36(12),1721-1735.
46. A.S. Fouda, H.M. El-Abbasy, A.A.Al-Sarawy, F.S. Ahmed, Corrosion inhibition of aluminum 6063 using some pharmaceutical compounds, Corrosion Science, 2009, 51(3), 485-492.
47. Y.Yan,W. Li,L.Cai,B. Hou, Electrochemical and quantum chemical study of purines as corrosion inhibitors for mild steel in 1 M HCl solution, Electrochimica Acta,2008, 53(20), 5953-5960.
48. A.Prithiba , Corrosion monitoring of metal Mild steel Aluminium 1M HCl interface in the presence of Spathodea campanulata Tecoma capensis leaf and flower extracts Chemical Electrochemical and Theoretical studies,shodhganga,2015, 200.
49. M.Prabakaran, S.H. Kim, V. Hemapriya, I.M. Chung, Evaluation of polyphenol composition and anti-corrosion properties of Cryptostegia grandiflora plant extract on mild steel in acidic medium, Journal of Industrial and Engineering Chemistry, 2016, 37, 47-56.
50. A.P.Hanza, R.Naderi, E.Kowsari,M.Sayebani, Corrosion behavior of mild steel in H 2SO4 solution with 1, 4-di [1′-methylene-3′-methyl imidazolium bromide]-benzene as an ionic liquid,Corrosion Science,2016, 107, 96-106.

51. A.A.Al-Amiery, F.A.B.Kassim, A. A. H. Kadhum, and A.B.Mohamad(2016) Synthesis and characterization of a novel eco-friendly corrosion inhibition for mild steel in 1 M hydrochloric acid, Sci Rep,1980, 6.
52. V. D'Antò, R. Rongo, G. Ametrano, G. Spagnuolo, P. Manzo, R. Martina, S. Paduano, and R. Valletta, Evaluation of surface roughness of orthodontic wires by means of atomic force microscopy,The Angle Orthodontist,2012, 82(5), 922-928S.
53. S. Lilliu,C. Maragliano, M. Hampton, M. Elliott,M. Stefancich,M. Chiesa,M. S. Dahlem,and J.E. Macdonald(2013) EFM data mapped into 2D images of tip-sample contact potential difference and capacitance second derivative, Sci Rep,2013, 3, 3352.
54. K. Haïdara, L. Zamir, QW. Shi, G. Batist(2006) The flavonoid Casticin has multiple mechanisms of tumor cytotoxicity action,Cancer letters,242(2),180-90.
55. H.Aghajani, and M.S. Motlagh, Effect of temperature on surface characteristics of nitrogen ion implanted biocompatible titanium, J Mater Sci Mater Med, 2017, 28(2), 29.
56. P.Muthirulan, N.Kannan, and M.Meenakshisundaram, Synthesis and corrosion protection properties of poly(o-phenylenediamine) nanofibers, J Adv Res,2013, 4(4), 385-392.
57. J.Narenkumar , P.Parthipan , A.U. R. Nanthini ,G. Benelli , K. Murugan,A. Rajasekar, Ginger extract as green biocide to control microbial corrosion of mild steel, 3 Biotech,2017, 7(2), 133.
58. N. Salvadó, S. Butí, A. Labrador, G. Cinque, H. Emerich, T. Pradell , SR-XRD and SR-FTIR study of the alteration of silver foils in medieval paintings, Anal Bioanal Chem,2011, 399(9),3041-52
59. N.S.I.Geweely, Evaluation of ozone for preventing fungal influenced corrosion of reinforced concrete bridges over the River Nile, Egypt, Biodegradation, 2011, 22(2), 243-252.
60. A.M. Atta , G.A. El-Mahdy , H.A. Al-Lohedan , A.M. El-Saeed , Preparation and application of crosslinked poly(sodium acrylate)--coated magnetite nanoparticles as corrosion inhibitors for carbon steel alloy, Molecules,2015, 20(1), 1244-61.
61. B.Stuart, Infrared spectroscopy: fundamentals and applications, JohnWiley & Sons, ,Ltd. 2004, ISBNs: 0-470-85427-8 (HB), 0-470-85428-6 (PB).

Corresponding author: A.S. Fouda

Chemistry Department, Faculty of Science, Mansoura University, Mansoura-35516, Egypt

asfouda@mans.edu.eg

Online publication Date: 29.07.2018